

Synthesis, Spectroscopic Characterization, and Anticancer Activity of Metal Complexes with a Novel Schiff Base Ligand from β -Diketone Derivatives

^{1,2}Ahmed N. Alhakimi*, ¹Thikra A. Almuhanha. ¹Jawza Sh. Alnawmasi
¹S. El-Sayed Saeed and ³Ebtesam Hassan L Alhamzi

¹ Department of Chemistry, College of Science, Qassim University, Buraidah-51452, Saudi Arabia.

² Department of Chemistry, Faculty of Science, Ibb University, Ibb, Yemen.

³ Department of Biology, College of Science, Sana'a University, Yemen.

A.Alhakimi@qu.edu.sa, alhakemi10@yahoo.com*

(Received on 15th November 2021, accepted in revised form 18th February 2022)

Summary: A new series complexes of Ni(II), Mn(II), Co(III), Cu(II), Cr(II), Zn(II), Zr(IV), Cd(II), and La(III) prepared by the reaction of the metal salt with a new Schiff base ligand. This Schiff base obtained by the condensation of p-phenylenediamine, 4-chlorobenzaldehyde, and acetyl acetone. The confirmation of the ligand and its metal complexes were characterized by multiple techniques such as, elemental analyses, magnetic susceptibility studies, FTIR ¹H, ¹³C-NMR, XRD, molar conductance, UV-vis spectral analyses, and thermal analyses. The conductivity measurements of the complexes in DMF solutions indicated that the prepared complexes are nonelectrolytes. From the spectral data, an octahedral geometry was suggested for all complexes. The metal complex [(L)₂Zr(Cl)₂].3H₂O showed the highest antifungal activity. The complexes [(L)(HL)Co(Cl)₂].3H₂O, and [(L)₂Cd(H₂O)₂] showed antibacterial activities higher than the other complexes. All complexes are exhibited potent fungicides and bactericides than the ligand. Complex [(L)₂Cd(H₂O)₂] exhibited considerable cytotoxicity against PC-3, SKOV3, and HeLa cells. The ligand C₁₈H₁₇N₂OCl (HL) showed strong toxicity towards PC-3, HeLa cells, and moderate toxicity against SKOV3 cells.

Keywords: Schiff bases complexes; β -diketone; Antimicrobial; anticancer.

Introduction

Organic compounds are distinguished by their widespread and diverse use, as well as their varied and interesting research applications. Schiff bases are one of those compounds that are well known for their significance in many of the studies that have been conducted on them. Schiff bases are formed through simple condensation reactions between primary amines with aldehydes, ketones to give compounds containing the highly active azomethine group (-C=N-). The lone pair electrons in (-C=N-) causes the Schiff base activity. Further, the carbon atom present adjacent to the nitrogen atom makes the lone pair of electrons on the nitrogen atom more stable and more effective when coordinated with metal ion during the formation of complexes. [1-5].

Various spectroscopic techniques were used to confirm the formation of Schiff bases during the preparation process. It is easy to detect the formation of Schiff bases because they contain a special azomethine group. In recent years, many metal complexes of Schiff bases applications appeared which used in several variable fields such as industrial [6-8], pharmaceutical [9-10], analytical [11], and antimicrobial. Due to their structural nature these compounds possess great efficacy against malaria, virus, diabetic, fungal, inflammatory, corrosion, cancer, HIV, antipyretic symptoms, and helminthic [12-15].

The coordination of some metals with Schiff base ligands may cause increasing in the bioactivity of these compounds [16-18]. Therefore, the development of mineral complexes of Schiff bases for using it in chemical medicines has attracted the attention of many chemists and medical researchers [18- 22].

In the industry, Metal complexes Schiff bases showed high efficiency when used as photovoltaic materials in solar energy devices, making them important compounds in the manufacture of renewable energy devices [1,2]. β -diketones compounds are characterized by their ability to coordinate with metal elements in a large way, forming stable hexagonal rings with high biological activity, in addition to forming molecules of structural diversity that make them of great importance in coordination supramolecular chemistry. Compounds consisting of primary aromatic amine linked to β -diketones compounds have very great importance also, as they showed their positive effect in many different fields such as insecticides, antioxidants, sunscreen, anti-cancer cells, antifungal, antimicrobial, and anthelmintic activities. On the pharmacological side, derivatives of β -diketone compounds showed their ability to inhibit HIV-integrase (1N) [23-25]. Several studies conducted on β -diketone compounds against cancer cells showed high efficacy [26-28]. On the other hand, its derivatives also have this unique feature. For

*To whom all correspondence should be addressed.

example, Curcumin contains β -diketones compounds, which is a spice that has a very effective property against many cancer cells. It also showed an inhibition in the formation of DMBA-DNA in live mammals and have application in textile and other different fields. The coordination of β -diketone compounds with metallic elements gives them high thermal and kinetic stability, in addition to increasing their biological activity because these elements have a great impact on many different microorganisms [28-30].

Acetylacetone Schiff base were synthesized by the condensation of acetylacetone with primary amine. They are used in inorganic field as chelating ligands for metal complexes preparation. This is because the donor atoms of oxygen and nitrogen flexibility. Recently, researchers focused on the preparation and characterization of complexes with acetylacetone Schiff base due to its wide range applications in medicinal field and its ability to bonding with metal ions, which is highly desirable. Due to variable bonding modes of it, promising have received considerable attention because of their variable bonding modes, hopeful biological effects, and structural variety [30-32].

Because of the broad applications of β -diketone Schiff base complexes, this study directed to synthesis new complexes of Ni(II), Mn(II), Co(III), Cu(II), Cr(III), Zn(II), Zr(IV), Cd(II), La(III) based on (E) -4 - ((4 - (((Z) -4-chlorobenzylidene) amino) phenyl) imino) pentan-2-one ligand. The structure of the prepared ligand and complexes was investigated with different analytical techniques. In addition, the work investigate the antimicrobial and anticancer of the prepared compounds.

Experimental

Materials

The chemicals utilised to synthesise the ligand (HL) and its complexes were of analytical grade and were used without further purification. Acetyl acetone, 4-chlorobenzaldehyde, and ethanol absolute, metal salts were supplied by Sigma-Aldrich (purity: 98 to 99.99%). The purity of the synthesised compounds were confirmed by thin layer chromatography (TLC).

Instrumental analysis

The (C, H and N) content in the obtained compounds was analyzed on VARIO EL III GERMANY at the Microanalytical center, Faculty of Science, Cairo University. Metal ion content was estimated using standard analytical method [33]. In Qassim University's Analytical laboratory, Saudi

Arabia the rest of analysis were carried. FTIR spectra of the ligand and the complexes were recorded by using an Cary 600 Agilent spectrometer (USA). The (^1H -, ^{13}C -) electronic magnetic resonance spectra was carried out on a Bruker 850 and 213 MHz FT-NMR spectrometer using DMSO- d_6 as solvent. The XRD patterns were measured on a RIGAKU ULTIMA IV. Molar conductance of metal complexes in DMF (10^{-3} M) were recorded using an Oakton Conductivity/DTS meter. The electronic absorption spectra were recorded in ethanol using (UV-1650PC) Shimadzu spectrometer. Magnetic susceptibilities of the metal complexes was measured by Sherwood Scientific balance by using the Gouy technique at room temperature using mercuric tetra thiocyanato cobaltate (II) as the standard of magnetic susceptibility. The diamagnetic correction was calculated by using Pascal's constant [34]. Thermal analysis carried by (DTG-60AH) Shimadzu DT-30 in air from 27 to 525 $^{\circ}\text{C}$ with a heating rate of 10 $^{\circ}\text{C}/\text{min}$.

Preparation of ligand, (E) -4 - ((4 - (((Z) -4-chlorobenzylidene) amino) phenyl) imino) pentan-2-one (HL)

A slowly dropwise of acetylacetone (0.1 g, 0.001 mol) was added to the round flask of ethanolic solution of p-phenylenediamine (0.108 g, (0.001 mol)) and 4-chlorobenzaldehyde (0.140 g, (0.001 mol)). The mixture was refluxed with stirred for 4 hours after that it cooled to room temperature. the product was filtered, washed with hot EtOH several times, and dried with a anhydrous CaCl_2 desiccator. Ligand (HL), $\text{C}_{18}\text{H}_{17}\text{N}_2\text{OCl}$ (Formula Weight, FW = 312.80), yield: 83 %, melting point (M.p.) 190.4 $^{\circ}\text{C}$, colour: yellow. Elemental anal %: calcd.: C, 69.21; H, 5.48; N, 8.96; Found: C, 69.10; H, 5.40; N, 8.78. IR, ν (cm^{-1}): 1607_(m), 1595_(m), 1562_(s), 1650_(s). ^1H -NMR (δ , ppm): 1.98–5.18 (s, 1H, $-\text{CH}_3$), 7.26–7.84 (s, 11H, aromatic protons), 8.45 (s, 1H, $\text{N}=\text{CH}$). ^{13}C - nuclear magnetic resonance (NMR): δ = 20.6, 29.81, 43.88 ($-\text{CH}_3$), 158.97 ($\text{HC}=\text{N}$), 122.26–150.4 (aromatic carbon), 43,88 ($-\text{CH}_2$). UV-vis (EtOH), λ_{max} (nm): 248, 350.

Preparation of metal complexes

All the complexes were synthesized by refluxing ethanolic solutions of the following salts while stirring for 4 h: $\text{NiCl}_2 \cdot 6\text{H}_2\text{O}$, $\text{MnCl}_2 \cdot 4\text{H}_2\text{O}$, $\text{CuCl}_2 \cdot 2\text{H}_2\text{O}$, $\text{CoCl}_3 \cdot 6\text{H}_2\text{O}$, $\text{CrCl}_3 \cdot 6\text{H}_2\text{O}$, ZnCl_2 , $\text{ZrCl}_4 \cdot \text{H}_2\text{O}$, $\text{CdCl}_2 \cdot \text{H}_2\text{O}$, and $\text{LaCl}_3 \cdot \text{H}_2\text{O}$ with suitable amounts of ethanolic ligand solution in a molar ratio of 1Metal: 2 Ligand in the presence of drops from triethylamine as a basic media. The formed precipitates filtered, washed by using with hot ethanol, and dehydrated by using anhydrous CaCl_2 desiccator.

Ni(II) complex (2). (FW = 734.11), yield: 72 %, M.p.> 300 °C. Colour: Dark green, molar conductance (Λ): $23.3 \Omega^{-1} \text{ cm}^2 \text{ mol}^{-1}$. Elemental analysis % . calcd.: C, 58.69; H, 4.79; N, 7.60; Ni, 7.97. Found: C, 58.60; H, 4.35; N, 7.52; Ni, 7.84. IR, v (cm^{-1}): 3313_(s), 3260_(br), 3100_(br), 1612_(m), 1508_(s), 1318_(s), 690_(s), 554_(s), 410_(s). UV-vis (EtOH), λ_{max} (nm): 336, 390, 643.

Mn(II) complex (3). (FW = 731.11), yield: 78 %, M.p.> 294 °C. Colour: Brown, Λ : $14.2 \Omega^{-1} \text{ cm}^2 \text{ mol}^{-1}$. Elemental analysis % . calcd.: C, 58.99; H, 8.81; N, 7.64; Mn, 7.50. Found: C, 58.80; H, 4.44; N, 7.51; Mn, 7.50. IR, v (cm^{-1}): 3335_(s), 3320_(br), 3100_(br), 1609_(m), 1550_(s), 1302_(s), 655_(s), 553_(s), 420_(s). UV-vis (EtOH), λ_{max} (nm): 321, 348, 480, 614.

Cu(II) Complex (4). (FW = 775.1), yield: 74 %, M.p.> 300 °C. Colour: Black, Λ : $9.2 \Omega^{-1} \text{ cm}^2 \text{ mol}^{-1}$. Elemental analysis % . calcd.: C, 55.57; H, 4.66; N, 7.20; Cu, 8.17. Found: C, 55.50; H, 4.66; N, 7.15; Cu, 8.10. IR, v (cm^{-1}): 3500_(br), 1635, 1605_(s), 1585_(m), 1650_(s), 1315_(s), 686_(s), 540_(s), 459_(s). UV-vis (EtOH), λ_{max} (nm): 281, 306, 352, 443.

Co(III) complex (5). (FW = 808.72), yield: 75 %, M.p.> 300 °C. Colour: Pale green, Λ : $19.3 \Omega^{-1} \text{ cm}^2 \text{ mol}^{-1}$. Elemental anal % . calcd.: C, 53.48; H, 4.86; N, 6.39; Co, 7.29. Found: C, 53.35; H, 4.77; N, 6.50; Co, 7.19. IR, v (cm^{-1}): 3411_(s), 3560_(br), 3250_(br), 1600, 1587_(m), 1562_(s), 1320_(s), 681_(s), 556_(s), 405_(s). UV-vis (EtOH), λ_{max} (nm): 251, 307, 400, 506.

Cr(III) complex (6). (FW = 763.13) , yield: 70 %, M.p.> 300 °C. Colour: Brown, Λ : $6.3 \Omega^{-1} \text{ cm}^2 \text{ mol}^{-1}$. Elemental anal % . calcd.: C, 57.88; H, 4.86; N, 7.50; Cr, 9.96. Found: C, 57.73; H, 4.82; N, 7.43; Cr, 6.87. IR, v (cm^{-1}): 3580_(br), 3180_(br), 1615, 1586_(m), 1563_(s), 1284_(s), 683_(s), 556_(s), 407_(s). UV-vis (EtOH), λ_{max} (nm): 293, 322, 464.

Zn(II) complex (7). (FW = 724.99), yield: 73 %, M.p.> 297 °C. Colour: Orange, Λ : $3.6 \Omega^{-1} \text{ cm}^2 \text{ mol}^{-1}$. Elemental anal % . calcd.: C, 59.64; H, 5.01; N, 7.73; Zn, 9.02. Found: C, 59.66; H, 5.01; N, 7.67; Zn, 9.00. IR, v (cm^{-1}): 3580_(br), 1614, 1595_(m), 1567_(s), 1310_(s), 643_(s), 537_(s), 422_(s). UV-vis (EtOH), λ_{max} (nm): 290, 300, 379.

Zr(IV) complex (8). (FW = 839.09), yield: 69 %, M.p.> 300 °C. Colour: Pale orange, Λ : $5.2 \Omega^{-1} \text{ cm}^2 \text{ mol}^{-1}$. Elemental anal % . calcd.: C, 51.49; H, 4.56; N, 6.67; Zr, 10.86. Found: C, 51.40; H, 4.47; N, 6.62; Zr, 10.82. IR, v (cm^{-1}): 3365_(s), 3300_(br), 1610, 1579_(m), 1547_(s), 1316_(s), 642_(s), 522_(s). UV-vis (EtOH), λ_{max} (nm): 255, 300, 345.

Cd(II) complex (9). (FW = 772.20), yield: 79 %, M.p.> 283 °C. Colour: Yellow, Λ : $4.6 \Omega^{-1} \text{ cm}^2 \text{ mol}^{-1}$. Elemental anal % . calcd.: C, 56.01; H, 4.70; N, 7.26; Cd, 14.56. Found: C, 56.06; H, 4.66; N, 7.20; Cd, 14.55. IR, v (cm^{-1}): 3230_(br), 3030_(br), 1612, 1602_(m), 1548_(s), 1314_(s), 615_(s), 5405_(s). UV-vis (EtOH), λ_{max} (nm): 235, 357, 397.

La(III) complex (10). (FW = 769.1) , yield: 67 %, M.p.> 290 °C. Colour: Dark orange, Λ : $5.4 \Omega^{-1} \text{ cm}^2 \text{ mol}^{-1}$. Elemental anal % . calcd.: C, 54.19; H, 4.04; N, 7.02; La, 17.41. Found: C, 54.18; H, 4.00; N, 6.95; La, 17.39. IR, v (cm^{-1}): 3300_(br), 3180_(br), 1613, 1600_(m), 1562_(s), 1301_(s), 620_(s), 555_(s), 455_(s). UV-vis (EtOH), λ_{max} (nm): 270, 316.

Antimicrobial effect

All the tests involving the antimicrobial activities of the complexes and ligand and its metal were performed at the Yemen Standardisation, Metrology, and Quality Control Organization and Althubhani Specialist Medical Laboratory, Sana'a-Yemen. The antibacterial activity assays of the compound were performed using the hole plate diffusion method [35,36]. The bacterial suspension (100 μl) was spread by a sterile cotton swab on plates containing Mueller-Hinton agar [37]. By using a cork borer, three holes of 5 mm diameter were then made in the agar plates using a cork borer. Ligand and the complexes at different quantities (30, 20, and 10 μl) were added into each of the holes of Petri dishes. The Gentamicin antibiotic with concentration of 10 / mg used as a positive control [38]. After that the plates were put at 37 °C for 24 h. After incubation, the inhibition zones diameter were measured in mm. The inhibition zones were performed to be the diameter of the zone visibly showing the absence of growth including the 5 mm each for well. If there were no inhibition zone, the value of 0 mm was marked to the test samples [39]. Under similar conditions, antifungal activities of the metal complexes solutions were examined. The fungal suspension (100 μ) was spread by cotton swab which it is a sterile on Sabouraud Dextrose Agar (SDA). Using a sterile micropipette, complexes at different quantities (30, 20 and 10 μl) were added into each petri dishes holes. Adjusted the microbial cultures were 10⁶ colony formation unit/ml a sterile normal saline solution. Clotrimazole (10 μg / ml) antibiotics used as the positive control. The plates were then put for 24 hours at 28 °C for yeasts growth. After that the inhibition zones were measured with the previous method of antimicrobial [39].

Cell culture

The American type Culture Collection (ATCC) provided the human cell lines, prostate adenocarcinoma (PC-3), ovarian adenocarcinoma (SKOV3), and cervical cancer (HeLa) cell lines. The cells were maintained with (10 % v/v) foetal bovine serum under a humidified condition with 5 % (v/v) CO₂. In RPMI-1640 medium containing 100 g/mL penicillin (100 units/L) it was incubated at 37 °C [40]. At 37 °C in RPMI-1640 supplemented with 100 g/mL penicillin (100 units/L) and heat-inactivated foetal bovine serum (10% v/v).

Cytotoxicity assay (Assay for cellular toxicity)

Investigation of cytotoxicity of the ligand and the complexes compounds was performed by using the SRB assay against the human tumour cells (PC-3, SKOV3, and HeLa). Prior to treatment with the chemical compounds, 80 % confluent proliferating cells were trypsinised and cultivated in a plate of 96 well tissue culture for 24 hours. Untreated cells (control) were added to the cells that were exposed to different six concentrations of each complex (1000, 10, 1, 0.1, and 0.01 g/ml). The cells were exposed to the doses for 72 hours before being fixed with TCA (10 % w/v) at 4 °C for 1 hour. After repeated washes, the cells were stained with 0.4 % (w/v) SRB solution for 10 min in the dark. Glacial CH₃COOH (1 % v/v) was used to remove any remaining discolouration. The cells stained with SRB dissolved in Tris-HCl after drying overnight, and then the intensity of the colour was quantified using a

microplate reader at 540 nm. To determine the IC₅₀ (the drug dose that reduces survival to 50 %), The correlation between the viability % of each tumour cell line and the corresponding chemical concentration was analysed using SigmaPlot 12.0 software [41].

Results and Discussion

Ligand (HL) was prepared by the reaction of ethanoic solution of 4-chlorobenzaldehyde and benzene-1,4-diamine with acetylacetone with molar ratio (1:1) molar ratio, as shown in bellow Scheme 1.

¹H and ¹³C- nuclear magnetic resonance spectra of the ligand

The signal corresponding to the amino group (-NH₂) of the *p*-phenylenediamine is absent indicating to the formation of Schiff base. The ¹H-NMR spectrum of Schiff base showed two signals at (2.00 and 2.03) ppm which are assigned to the protons of methyl groups (-CH₃). The protons of methylene group (-CH₂) in precursor acetylacetone which was expected to appear as singlet at 3.3 ppm is absent indicating that Schiff base reacted to metal ions in its enolic form. This conclusion was confirmed by the appearance of a singlet at 5.26 ppm indicates to a proton of (C=CH) group in enolic acetyl acetone moiety and a singlet at 12.47 corresponding to the hydroxyl group of (OH) enolic acetyl acetone moiety. The multiple signals in the region 6.75–7.18 ppm was assigned to the phenyl protons while the singlet at 8.72 ppm was assigned to the azomethine proton (HC=N).

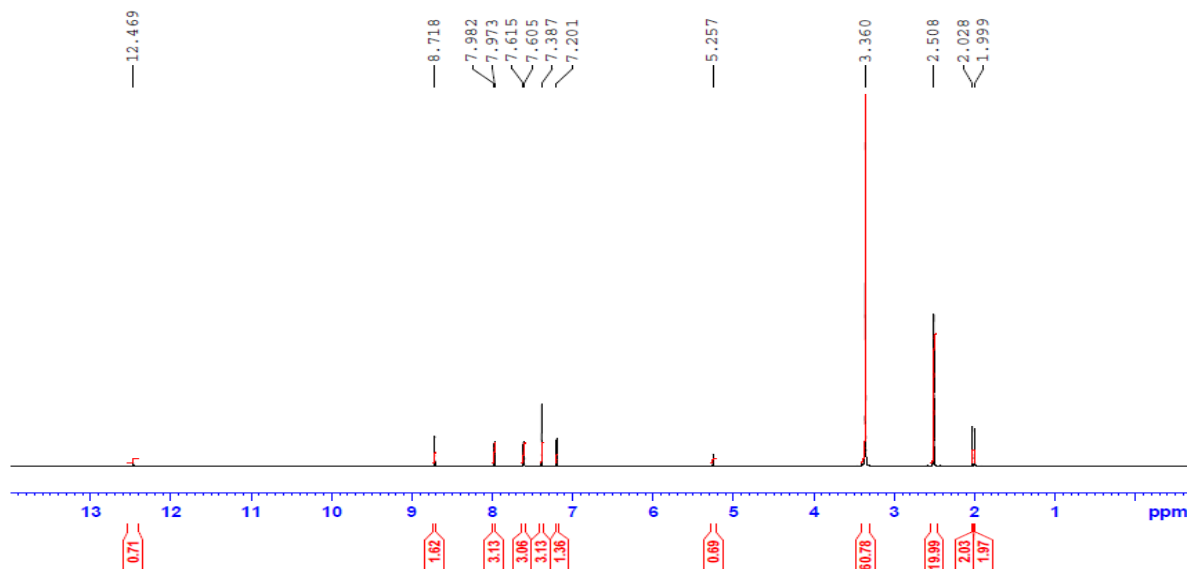


Fig. 1: ¹H-NMR spectrum of HL.

Table-1: Physical properties and elemental analyses of ligand and its metal complexes.

Comp. No.	Molecular Formula (m.w)	Color	Yield (%)	m.p. (°C)	$\Omega^{-1} \text{ mol}^{-1} \text{ cm}^2$	μ_{eff} (μB)	Found (Calc.) (%)			
							C	H	N	M
1	[HL][C ₁₈ H ₁₇ N ₂ OCl] (312.80)	Yellow	83	190.4	-	-	69.12 (69.10)	5.48 (5.40)	8.96 (8.78)	-
2	[(L)(HL)Ni(Cl)(H ₂ O)].3H ₂ O (734.113)	Dark Green	72	>300	13.3	2.50	58.69 (58.60)	4.79 (4.35)	7.64 (7.52)	7.97 (7.84)
3	[(L)(HL)Mn(Cl)(H ₂ O)].3H ₂ O (731.11)	Brown	78	294	14.2	3.40	58.99 (58.80)	4.81 (4.44)	7.64 (7.51)	7.50 (7.50)
4	[(HL) ₂ Cu(Cl) ₂].H ₂ O (775.1)	Black	74	>300	9.2	1.63	55.57 (55.50)	4.66 (4.66)	7.20 (7.15)	8.17 (8.10)
5	[(L)(HL)Co(Cl) ₂].3H ₂ O (808.72)	Pale Green	75	>300	19.3	4.60	53.48 (53.35)	4.86 (4.77)	6.39 (6.50)	7.29 (7.19)
6	[(L) ₂ Cr(Cl)(H ₂ O)].2H ₂ O (763.13)	Brown	70	>300	6.3	3.90	57.88 (57.73)	4.86 (4.82)	7.50 (7.43)	6.96 (6.87)
7	[(L) ₂ Zn(H ₂ O) ₂] (724.99)	Orange	73	297	3.6	Dia.	59.64 (59.66)	5.01 (5.01)	7.73 (7.67)	9.02 (9.00)
8	[(L) ₂ Zr(Cl) ₂].3H ₂ O (839.09)	Pale Orange	69	>300	5.2	Dia.	51.49 (51.40)	4.56 (4.47)	6.67 (6.62)	10.86 (10.82)
9	[(L) ₂ Cd(H ₂ O) ₂] (772.20)	Yellow	79	283	4.6	Dia.	56.01 (56.06)	4.70 (4.66)	7.26 (7.20)	14.56 (14.55)
10	[(L) ₂ La(Cl)(H ₂ O)] (769.1)	Dark Orange	67	290	5.4	Dia.	54.19 (54.18)	4.04 (4.00)	7.02 (6.95)	17.41 (17.39)

Table-2: UV-Vis. spectra of the ligand (HL), (1) and its metal complexes.

Comp. No.	Molecular formula	λ_{max} (nm)	molar extinction coef.(ϵ)
1	[HL][C ₁₈ H ₁₇ N ₂ OCl]	248, 350	$2.4 \times 10^{-2} \text{ mol}^{-1} \text{ cm}^{-1}$, $6.7 \times 10^{-2} \text{ mol}^{-1} \text{ cm}^{-1}$
2	[(L)(HL)Ni(Cl)(H ₂ O)].3H ₂ O	290, 357, 390, 643	$1.6 \times 10^{-4} \text{ mol}^{-1} \text{ cm}^{-1}$, $3.1 \times 10^{-4} \text{ mol}^{-1} \text{ cm}^{-1}$, $2.7 \times 10^{-3} \text{ mol}^{-1} \text{ cm}^{-1}$
3	[(L)(HL)Mn(Cl)(H ₂ O)].3H ₂ O	248, 360, 480, 614	$2.7 \times 10^{-4} \text{ mol}^{-1} \text{ cm}^{-1}$, $1.2 \times 10^{-4} \text{ mol}^{-1} \text{ cm}^{-1}$, $3.4 \times 10^{-3} \text{ mol}^{-1} \text{ cm}^{-1}$
4	[(HL) ₂ Cu(Cl) ₂].H ₂ O	236, 281, 352, 443	$3.2 \times 10^{-4} \text{ mol}^{-1} \text{ cm}^{-1}$, $2.1 \times 10^{-3} \text{ mol}^{-1} \text{ cm}^{-1}$
5	[(L)(HL)Co(Cl) ₂].3H ₂ O	251, 307, 400, 506	$1.1 \times 10^{-4} \text{ mol}^{-1} \text{ cm}^{-1}$, $4.8 \times 10^{-3} \text{ mol}^{-1} \text{ cm}^{-1}$
6	[(L) ₂ Cr(Cl)(H ₂ O)].2H ₂ O	293, 322, 464	$5.2 \times 10^{-4} \text{ mol}^{-1} \text{ cm}^{-1}$, $3.1 \times 10^{-3} \text{ mol}^{-1} \text{ cm}^{-1}$
7	[(L) ₂ Zn(H ₂ O) ₂]	248, 290, 300, 350	intraligand transitions
8	[(L) ₂ Zr(Cl) ₂].3H ₂ O	255, 300, 345, 400	intraligand transitions
9	[(L) ₂ Cd(H ₂ O) ₂]	235, 300, 350	intraligand transitions
10	[(L) ₂ La(Cl)(H ₂ O)]	270, 316, 350, 410	intraligand transitions

Table-3: Assignments of the diagnostic bands in the IR spectra of the ligand (HL), (1) and its metal complexes.

No.	OH/H ₂ Ohydr. /H ₂ Ocoord.	$\nu(\text{C}=\text{O})$	$\nu(\text{C}=\text{N})$	$\nu(\text{C}=\text{C})_{\text{Ar}}$	$\nu(\text{C}-\text{O})$	$\nu(\text{M}-\text{O})$	$\nu(\text{M}-\text{N})$	$\nu(\text{M}-\text{Cl})$
1	-	1650	1607, 1595	1562	-	-	-	-
2	3313 _(s) /3520-3260 _(br) /3240-3050 _(br)	-	1612, 1581	1508	1318	690	554	410
3	3335 _(s) /3560-3320 _(br) /3280-3100 _(br)	-	1609, 1595	1550	1302	655	553	420
4	-/3500-3320 _(br) /-	1655, 1650	1635, 1605	1585	1315	686	540	450
5	3411 _(s) /3560-3250 _(br) /-	-	1600, 1587	1562	1320	681	556	405
6	-/3580-3250 _(br) /3180-3080 _(br)	-	1615, 1586	1563	1284	683	556	407
7	3365 _(s) /-/3300-3230 _(br)	-	1610, 1579	1547	1316	642	522	-
8	-/3580-3290 _(br) /-	-	1614, 1595	1567	1310	643	537	422
9	-/3230-3030 _(br)	-	1612, 1602	1548	1314	615	405	-
10	-/3300-3180 _(br)	-	1613, 1600	1562	1301	620	555	455

The ¹³C- nuclear magnetic resonance spectra (Fig. 2) exhibited chemical shifts at 20.6, 29.81, and 43.88 ppm related to the carbon atoms of the CH₃ group located at the distal side of the carbonyl group, CH₃ in the position alpha to the carbonyl group, and -CH₂ in acetylacetone, accordingly [5,7,8]. The chemical shift at 158.97 ppm may be attributed to the carbon atom in the HC=N group [8]. The chemical shifts in the 122.26–150.4 ppm range correspond to the aromatic carbons [9,11]. The chemical shift at 43.88 ppm was attributed to the carbon atom of -CH₂ [11]. All complexes were solids, intensely coloured, stable at room temperature, and prolonged storage

did not decompose it. All complexes were soluble in polar solvents, such as EtOH, DMF and DMSO. The results of elemental analyses and data on the physical characteristics (Table-1), whilst the spectral data (Table-2 and 3). But unfortunately, we have not obtained crystals of the prepared compounds. However, we are making continued efforts to obtain crystals of the various complexes.

Conductivity Measurements

Molar conductance of the complexes in (10⁻³M) DMF were in the range of 3.6–19.3 $\Omega^{-1} \text{ cm}^2 \text{ mol}^{-1}$, as

listed in Table-1. Low values of the conductivity indicate that all complexes non-electrolytic in the nature [42].

Magnetic Moment

According to the results of magnetic moment measurements at room temperature, complexes 2–6 were found to be paramagnetic (Table 1). The Ni(II) complex (2) shows 2.51 B.M. magnetic moment value which is appropriate by way of octahedral Ni(II) complexes having two unpaired electron systems [43]. The complex of Mn(II) (3) shows 3.4 B.M. magnetic moment which less than the expected value may be due to electron – electron interaction, this value recommends an octahedral geometry around the Mn(II) ion [44]. The Cu(II) complex (4) shows 1.63 B.M. value. This is compatible with a system consisting of a single electron in an octahedral environment [45]. The Co(III) complex (5) shows 4.61 B.M. with high magnetic moment value, indicating that it is a high-spin Co(III) complex [46]. The Cr(III) complex (6) shows 3.9 B.M. with high magnetic moment value, which is characteristic of high-spin octahedral Cr(III) complexes [47]. Another complexes Zn(II) (7), Zr(IV) (8), Cd(II) (9), and La(III) (10) complexes are diamagnetic [44].

Electronic Spectra

The ligand (HL) and its metal complexes electronic spectral data in EtOH solutions are showed in Table-2. The ligand exhibited absorption bands at 350 and 248 nm due to the $n \rightarrow \pi^*$ and $\pi \rightarrow \pi^*$ transitions, accordingly, within the aromatic rings in the ligand Fig. 3 and 4. The DFT reveals the energy and dipole moment in the ligand equal -1419.11915160 au and 3.9260 Debye respectively. Table-2 showed that the complex of Ni(II) (2) exhibited bands at 357, 390, and 643 nm, which were assigned to the ${}^3A_{2g} \rightarrow {}^3T_{2g}(P)$, ${}^3A_{2g} \rightarrow {}^3T_{1g}(F)$, ${}^3A_{2g} \rightarrow {}^3T_{2g}(F)$ transitions accordingly, indicating an octahedral geometry around Ni(II) [45]. The Mn(II) complex (3) showed three bands at 361, 482, and 616 nm assigned to the ${}^4T_{1g}(D) \rightarrow {}^6A_{1g}$, ${}^4T_{2g}(G) \rightarrow {}^6A_{1g}$, and ${}^4T_{1g} \rightarrow {}^6A_{1g}$ transitions, respectively, which was compatible with an octahedral structure around Mn(II) [48]. The Cu(II) complex (4) showed bands at 443 and 352 nm, which are corresponding to the ${}^2B_{1g} \rightarrow {}^2B_{1g}$ and ${}^2B_{1g} \rightarrow {}^2A_{1g}$, transitions, respectively, suggesting a distorted octahedral [48]. The Co(III) complex (5) displayed bands at 980, 610, and 540 nm, which were attributed to the ${}^4T_{1g}(F) \rightarrow {}^4T_{2g}(F)$, ${}^4T_{1g}(F) \rightarrow {}^4A_{2g}(F)$, ${}^4T_{1g}(F) \rightarrow {}^4T_{2g}(P)$ and transitions, respectively, indicating a high-spin octahedral Co(III)

complex. The Cr(III) complex (6) displayed three bands at 293, 322, and 464 nm corresponding to the ${}^4A_{2g}(F) \rightarrow {}^4T_{1g}(F)$, ${}^4A_{2g}(F) \rightarrow {}^4T_{2g}(F)$, and ${}^4A_{2g}(F) \rightarrow {}^4T_{1g}(P)$ transitions, respectively, indicating an octahedral geometry around Cr(III) [47]. The transitions for the Zn(II) (7), Zr(IV) (8), Cd(II) (9), and La(III) (10) complexes are shown in Table-2. These complexes exhibit intra-ligand transitions [48, 49].

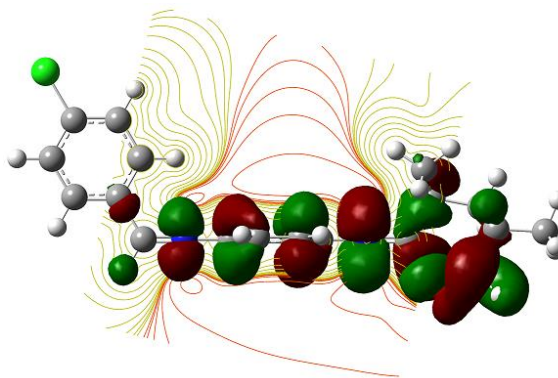


Fig. 3: HOMO orbital of ligand (HL).

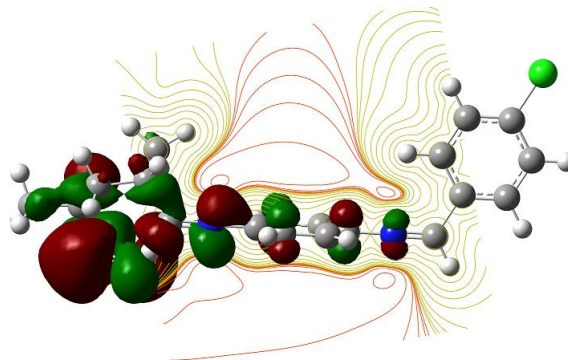


Fig. 4: LUMO orbital of ligand (HL).

FTIR spectra

FTIR spectra of the ligand and its metal complexes showed different bands, which were listed in Table-3. The spectra of the ligand showed in (3510–3200) cm^{-1} range broad medium bands, related to inter and intramolecular hydrogen bonds. Also other bands at 1650, 1607, 1595, and cm^{-1} , related to secondary $\nu(\text{C}=\text{O})$ and $\nu(\text{C}=\text{N})$, respectively [50, 5, 7]. In addition, the band at 1562 cm^{-1} , corresponds with $\nu(\text{C}=\text{C})_{\text{aromatic}}$ (aromatic C=C stretching). To ascertain the process of coordination between the metal ions and the ligand, the IR spectrum of them were compared. The complexes showed broadband between the range (3580–3100) cm^{-1} due to the occurrence of coordinated or hydrated H_2O molecules

or hydroxyl group, which subscribe to (inter or intramolecular) hydrogen bonding in the complexes 2–10. The complexes 2, 3, 5, and 8 were shown were strong bands at 3313, 3335, 3411, and 3365 cm^{-1} respectively indicate the presence of a hydroxyl group (-OH) in the complexes. All the complexes except 7, 9, and 10 displayed a broad band between 3580–3250 cm^{-1} , related to hydrated water molecules. Except for complexes 4, 5, and 8, a brooded band appears in the 3300–3030 cm^{-1} range due to coordinated water molecules [6]. The only complex 4 which in (1655–1650) cm^{-1} range showed a strong band (Table-3), which is related to $\nu(\text{C}=\text{O})$ [5,7,9]. However, medium and strong bands appeared in the 1635–1579 and 1585–1508 cm^{-1} ranges, which were related to $\nu(\text{C}=\text{N})$ and $\nu(\text{C}=\text{C})_{\text{Ar}}$, respectively [7-9,11]. The medium band which appeared in (1320–1284) cm^{-1} range corresponds to $\nu(\text{C}-\text{O})$ [11]. All the complexes except 8 and 9 showed a medium band in the 455–405 cm^{-1} range, corresponding to the terminal and bridging chloride ions. The complexes showed weak bands in the 690–620 and 556–504 cm^{-1} ranges due to the metal- ligand bonding with through O and N atoms, which are attributed to $\nu(\text{M}-\text{O})$ and $\nu(\text{M}-\text{N})$, correspondingly [10,11].

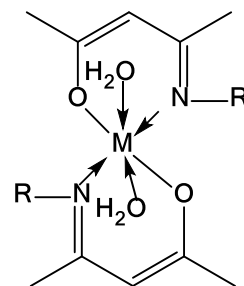
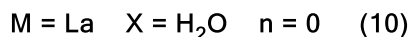
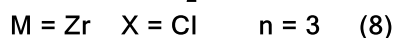
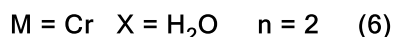
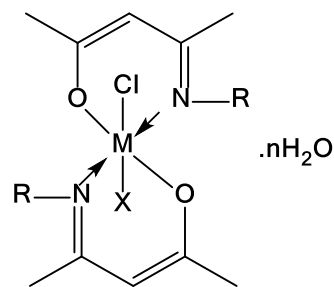
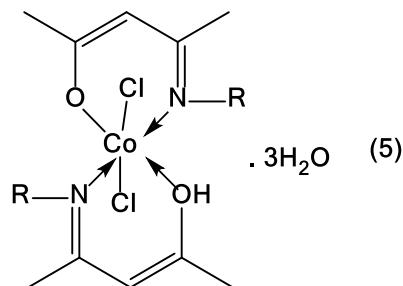
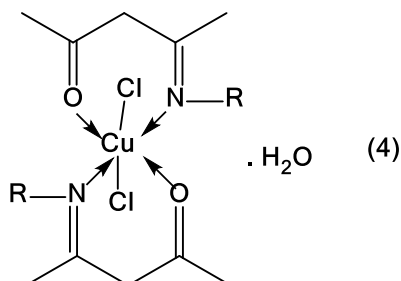
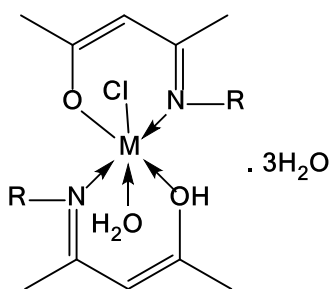
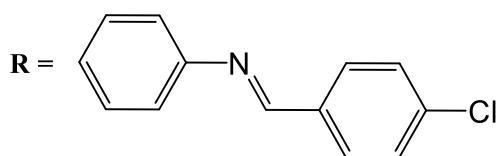


Fig. 5: The representation structural of the complexes.

Thermal analysis

Schiff base ligand (HL) and the metal complexes thermal analysis performed in order to learn about its thermal stability. Also, to confirm whether the status of the water inside or outside the central metal ion coordination spheres. The thermogravimetric analysis (TGA) curves in the range of 27–800 °C indicate stability of the complexes up to 50 °C. The TGA results of some complexes matched the elemental analysis formula. The TGA data clearly showed that the complexes were decomposed in sequential processes [5-8].

Table-4: XRD data of complexes.

Comp. No.	a (Å)	b (Å)	c (Å)	α (°)	β (°)	γ (°)	Cell Volume (Å ³)	Crystal size (Å)	Crystal type	Space group
2	9.474	8.715	14.356	90.06	99.96	90.06	1075.5	31.0	monoclinic	P2/m
3	4.336	4.336	14.487	90.00	90.00	90.00	272.44	20.5	Tetragonal	P4
4	24.39	12.47	7.63	90.00	90.00	90.00	2320	10.8	orthorhombic	P2
5	7.294	8.536	3.567	90.00	97.51	90.00	220.2	14.2	monoclinic	C2/m
6	5.668	14.97	5.280	90.00	90.00	90.00	448.1	204.9	Orthorhombic	P2
7	11.617	25.241	4.633	90.00	90.00	90.00	1358	185	Orthorhombic	P2
8	21.085	10.01	13.99	90.00	96.20	90.00	2714	86	monoclinic	P2
9	19.34	9.85	9.43	90.00	102.1	90.00	1758	30.9	monoclinic	P2
10	5.351	5.351	13.08	90.00	90.00	100.00	1224.3	113	hexagonal	P6

Complexes **2**, **3**, and **6** decayed in four steps. The 1st step occurred at 60–120 °C with losses of 6.38, 6.85, and 6.39 % (calcd. 6.20, 6.71, and 6.29 %, respectively) because of the sequential removal of hydrated water (3H₂O) molecules. The 2nd step happened in the 122–185 °C range with weight losses of 2.27, 2.28, and 2.34% (calcd. 2.32, 2.21, and 2.41%, respectively) as due to the elimination of coordinated H₂O molecules. The 3rd stage happened in range of 189–320 °C with losses of 4.49, 4.50, and 4.63 weight % (calcd 4.53, 4.39, and 4.61 %, respectively) corresponding to chlorine removal. The final stage occurred at (520, 500 and 620) to (720, 750 and 750) °C range with weight losses of 76.96, 77.37, and 79.48 % (calcd. 75.63, 77.8, and 79.1% of the remaining material respectively) for each of the three complexes respectively, corresponding to the complexes' full degeneration and transformation to metal oxides (NiO, MnO₂ and CrO₃) respectively. Complexes **4**, **5**, and **8** decomposed in three steps. At a temperature range 75–140 °C, the first step occurred with weight loss of 2.31, 6.39, and 6.42 % (calcd. 2.42, 6.26, and 6.51 %, respectively) due to the removal of hydrated H₂O. The 2nd stage happened at a temperature range 153–310 °C with weight losses of 9.13, 12.61, and 8.44 % (calcd. 10.07, 11.41, and 9.96 %, respectively) due to the removal of chlorine. The 3rd step happened in the (520, 650 and 520) to (750, 750 and 750)°C range with weight losses of 78.33, 72.13, and 72.4 % (calcd. 74.01, 70.01, and 70.19 %, of the remaining material respectively) relating to the complexes' degeneration and transformation to metal oxides (CuO, Co₂O₃ and ZrO₂) respectively. Complexes **7** and **9** decayed in two steps. At a temperature range 130–195 °C, the first step happened with weight losses of 4.95 and 4.65 % (calcd. 5.54 and 4.35 %, respectively) owing to the coordinated (2H₂O) molecules removal. The 2nd stage happened in (650, and 750) to (750, and 800) °C range with losses of 83.85 and 78.75 weight % (calcd. 82.6 and 77.87 %, of the remaining material respectively) related to the complexes complete decomposition and transformation to metal oxides (ZnO and CdO) respectively. Complex **10** was decayed in 3 steps. The 1st step occurred at 130 °C with a 2.2 % loss of weight (calcd. 2.84 %), related to the loss of H₂O coordinated molecule. The 2nd step happened in the temperature range of 220–310 °C with a

4.34 % loss of weight (calcd. 4.41%) related to the elimination of chloride. The 3rd step happened in the 450–750 °C range with a 74.51 % loss of weight (calcd. 75.12 % of the remaining material) corresponding to the complex's complete degeneration and transformation to metal oxide La₂O₃ [8, 9, 44, 45].

XRD analysis

The XRD measurement output data was processed and enhanced utilizing software. The crystal structure data of the complexes matched with the crystal systems. The complexes parameters of the unit cell are listed in Table-4. The differences in computed unit cell volumes were caused by the sizes of the impurities present in the base material. Notably, complexes 2, 5, 8, and 9 exhibit monoclinic crystal systems. Complex 4, whose XRD spectrum is shown in Fig. 6 (a), has a tetragonal crystal system. Complexes 4, 6 and 7 have orthorhombic crystal systems. A hexagonal crystal system was observed for complex 10, whose XRD spectrum is shown in Fig. 6 (b) [10].

Antibacterial activities of complexes at different volumes against the growth of *Salmonella typhi*

The data in Fig. 7 represent the antibacterial activities of the complexes at different volumes against the growth of *Salmonella typhi*. Complexes 5, 7, and 8 had high antibacterial activities against *S. typhi* at their levels (30 and 20 µl), while they had intermediate antibacterial activities against *S. typhi* at their level (10 µl) (Fig. 7 and 8). Complexes 2, 4, and 6 had intermediate antibacterial activities against *S. typhi* at their levels (30, 20, and 10 µl). Complex 9 had intermediate antibacterial activity against *S. typhi* at its levels (30 and 20 µl) while its activity was small against *S. typhi* at their level (10 µl). Complex 3 had weak antibacterial activity against *S. typhi* at their levels (30, 20, and 10 µl). Complex 10 showed small antibacterial activity opposed to *S. typhi* at their level (30 µl). On the other hand, HL did not exhibit any antibacterial activity against *S. typhi* at their levels (30, 20, and 10 µl). In this study Gentamycin 10µg was used as positive control [51-54].

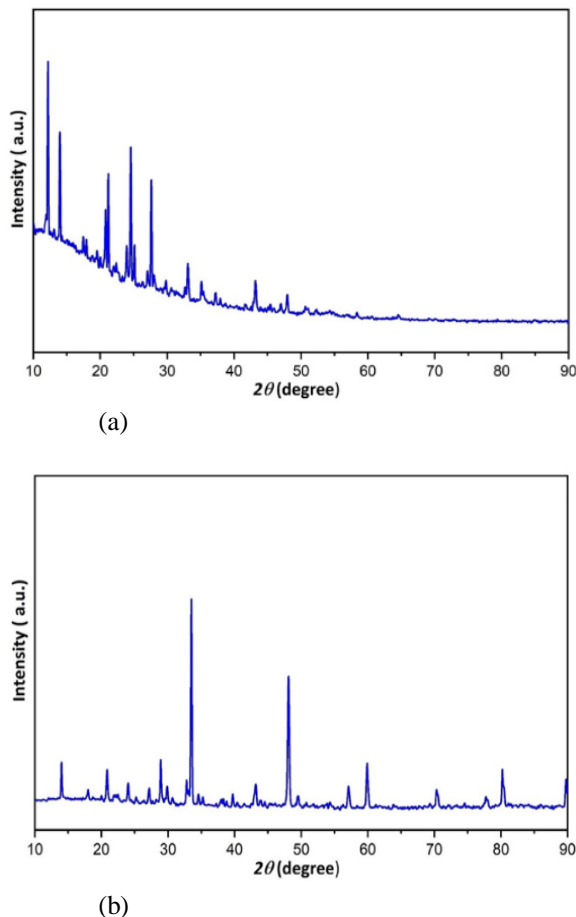


Fig. 6: XRD for Complexes (a) Cu(II) complex and (b) La(III) complex

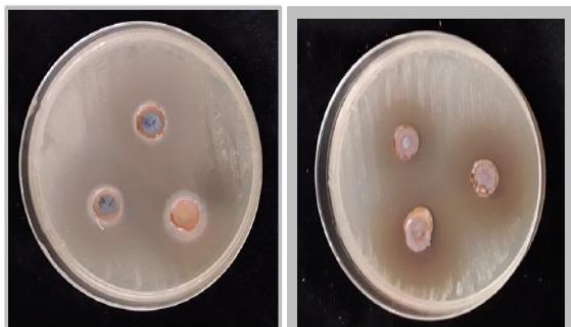


Fig. 7: Inhibition zones of complex on bacteria.

Antifungal activities of complexes at different volumes against growth of Candida albicans

The results in Fig. 9 correspond to the antifungal activities of the complexes at different volumes against the growth of *C. albicans*. Cadmium complex (9) had the highest activity against *C. albicans* at their levels (30, 20, and 10 μ l) (Fig.

10). Complexes of nickel (2), cobalt (5), Chrome (6), and zinc (7) showed a high antifungal activities against *C. albicans* at their levels (30, 20, and 10 μ l). Zirconium complex (8) had the highest antifungal activity against *C. albicans* at their levels (30 and 20 μ l), while they had intermediate antifungal activities against *C. albicans* at their levels (10 μ l) (Fig. 9). Copper complex (4) had intermediate antifungal activity against *C. albicans* at their levels (30 and 20 μ l), while they had weak antifungal activities against *C. albicans* at their levels (10 μ l). HL had weak antifungal activity against *C. albicans* at their levels (30 and 20 μ l). Manganese Complex (3) showed weak antifungal activities against *C. albicans* at their levels (30, 20, and 10 μ l). On the other hand, Lanthanum complex (10) did not have any antifungal activity against *C. albicans* at their levels (30, 20, and 10 μ l) [51-54].

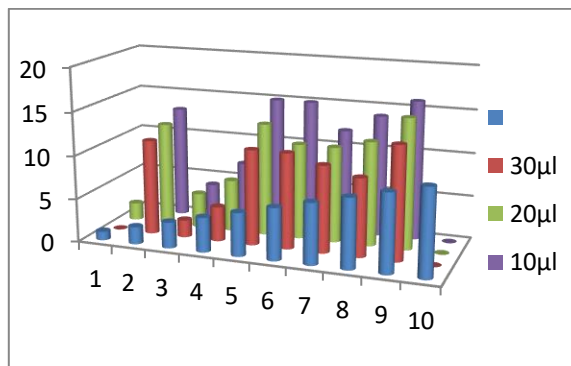


Fig. 8: Antibacterial activities of different levels of ligand and complexes against growth of *S. typhi*.

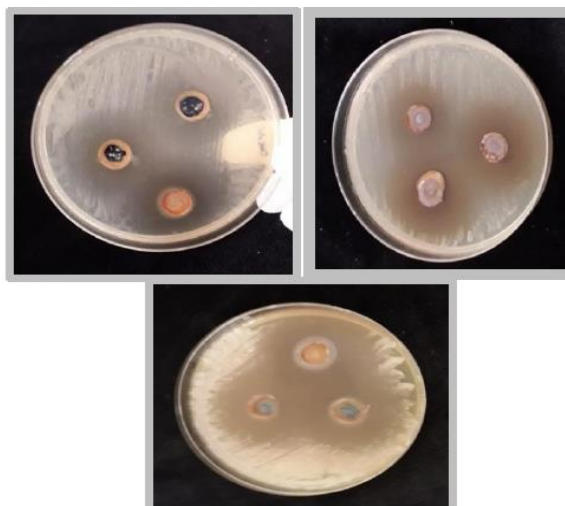


Fig. 9: Inhibition zones of complex on Fungal.

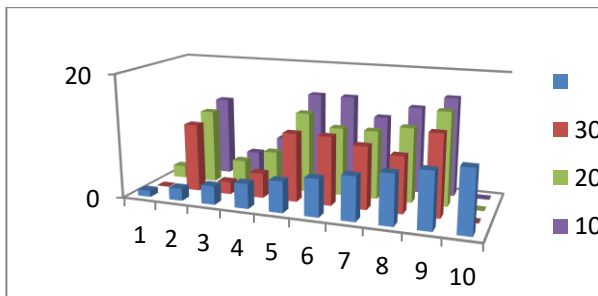


Fig. 10: Antifungal activities of complexes at different volumes against growth of *Candida albicans*.

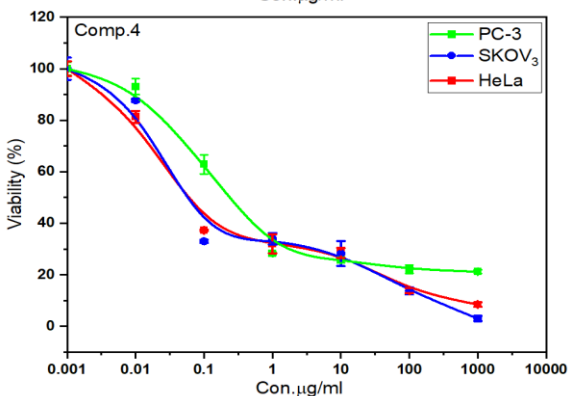
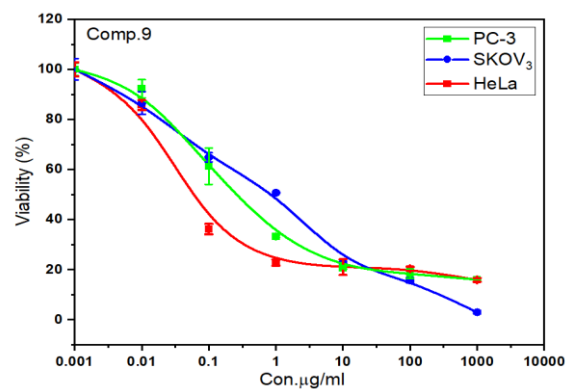
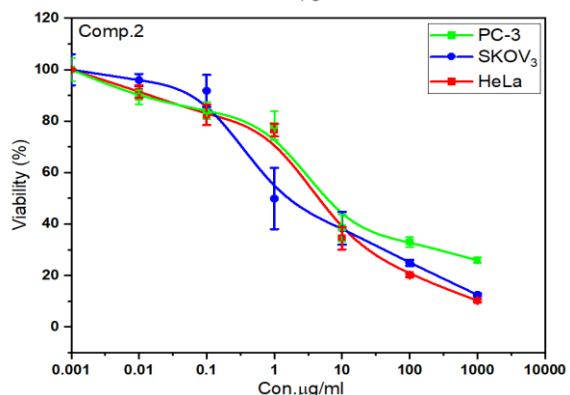
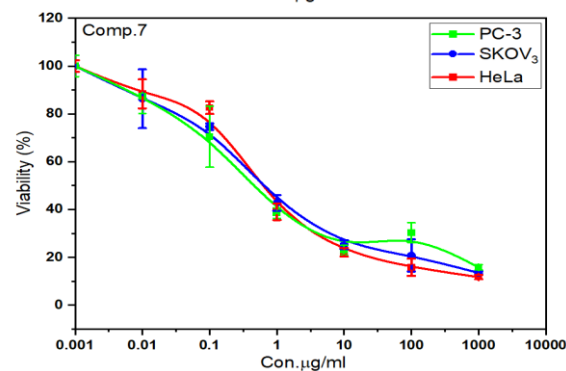
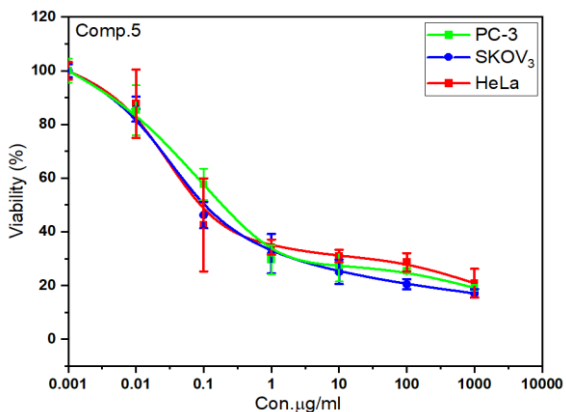
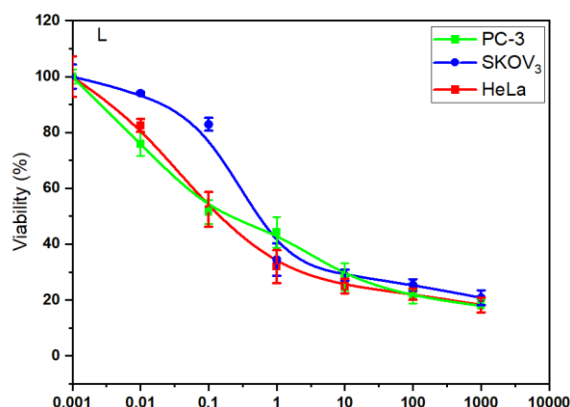


Fig. 11: The dose response curves of the cytotoxicity of different compounds towards PC-3, SKOV3, and HeLa tumour cell lines.

Anticancer activities

The prepared compounds in vitro cytotoxic activities determined by using the sulforhodamine B (SRB) assay for MCF-7, HCT 116, and HepG2 tumour cell lines over a range of concentration 0.01 to 1000 µg. The investigated compounds showed variable activity towards human tumour cells. The most toxicity was observed with the Cd(II) complex towards PC-3, SKOV3, and HeLa cells with IC₅₀ values of 0.4 ,

0.7, and 0.43, respectively. The ligand HL exhibited moderate toxicity towards SKOV3 tumour cells with an IC₅₀ value of 1.46 and high toxicity against PC-3 and HeLa cells with IC₅₀ values of 0.29 and 0.30 µg, correspondingly (Fig. 11). In addition, the Cu(II) complex exhibited the strongest toxicity towards cancer (SKOV3 and HeLa) cells among all the compounds, with IC₅₀ values of 0.15 and 0.18 µg, correspondingly. The Mn(II) complex showed strong toxicity towards cancer (SKOV3) cells with an IC₅₀ value of 0.7 µg. The Co(III) and Zn(II) complexes exhibited strong toxicity towards cancer (PC-3) cells with IC₅₀ values of 0.93 and 0.92, correspondingly. On the other hand, the Ni(II) complex was weaker at killing PC-3 cells and had moderate cytotoxicity towards SKOV3 cells and a significant cytotoxic effect on HeLa cells, with IC₅₀ values of 11.3, 3.66, and 4.41 µg, correspondingly (Table-5) [55-57].

Table-5: The IC₅₀ (µg) of the tested ligand and its metal complexes against different tumour cell lines.

Comp. No.	Molecular formula	IC ₅₀ (µg)		
		PC-3	SKOV3	HeLa
1	[HL][C ₁₈ H ₁₇ N ₂ OCl]	0.30 ± 0.08	1.46 ± 0.26	0.29 ± 0.05
		0.51	1.09	0.28
2	[(L)(HL)Ni(Cl)(H ₂ O)] ₂ ·3H ₂ O	4.41 ± 0.51	3.66 ± 1.09	11.3 ± 0.28
		0.18	0.08	0.09
3	[(L)(HL)Mn(Cl)(H ₂ O)] ₂ ·3H ₂ O	2.79 ± 0.18	0.76 ± 0.08	1.35 ± 0.09
		0.18 ± 0.09	0.15 ± 0.01	0.53 ± 0.02
4	[(HL) ₂ Cu(Cl) ₂] ₂ ·H ₂ O	0.93 ± 0.08	0.27 ± 0.04	0.31 ± 0.07
		0.09	0.01	0.02
5	[(L)(HL)Co(Cl) ₂] ₂ ·3H ₂ O	0.93 ± 0.08	0.27 ± 0.04	0.31 ± 0.07
		0.09	0.01	0.02
7	[(L) ₂ Zn(H ₂ O) ₂]	0.92 ± 0.06	0.86 ± 0.17	0.86 ± 0.04
		0.06	0.17	0.04
9	[(L) ₂ Cd(H ₂ O) ₂]	0.43 ± 0.13	0.77 ± 0.04	0.44 ± 0.02
		0.13	0.04	0.02

Conclusion

The studied ligand behaves as anionic or neutral chelating with the ions of the studied metal elements. Also, the prepared complexes did not show any ionic behavior when their molar conductivity was measured using DMF solvent. The ligand and the complexes showed a clear effect on Salmonella typhi bacteria and C. albicans fungi in varying proportions. The ligand HL exhibited moderate toxicity against human tumor cells. The investigated compounds exhibited variable cytotoxic activity against human tumor cells. The most remarkable toxicity was observed for Cd(II) complex against PC-3, SKOV3, and HeLa cells, while the Cu(II) complex exhibited the strongest toxicity towards cancer (SKOV3 and HeLa) cells among all the compounds.

References

1. A. Jeevadason, Wesley, K. K. Murugavel, and M. A. Neelakantan. "Review on Schiff bases and their metal complexes as organic photovoltaic materials." *Ren. and Sust. Ener. Rev.* **36** (2014).
2. L. X., C. Manzur, N. Novoa, S. Celedón, D. Carrillo, and J. R. Hamon. "Multidentate unsymmetrically-substituted Schiff bases and their metal complexes: Synthesis, functional materials properties, and applications to catalysis." *Coord. Chem. Rev.* **357** (2018).
3. A. Dief, M. Ahmed, and MA. Ibrahim Mohamed. "A review on versatile applications of transition metal complexes incorporating Schiff bases." *Beni-suef univ. j. of basic and appl. sci.* **4**, 2 (2015).
4. W. Al Zoubi, , A. A. Salih Al-Hamdani, and M. Kaseem. "Synthesis and antioxidant activities of Schiff bases and their complexes: a review." *Appl. Organ. Chem.* **30**, 10 (2016).
5. A. Saad El-Tabl, , F. A. El-Saied, W. Plass, and A. Noman Al-Hakimi. "Synthesis, spectroscopic characterization and biological activity of the metal complexes of the Schiff base derived from phenylaminoacetohydrazide and dibenzoylmethane." *Spect. chim. Acta Part A: Mol. and Bio. Spect.* **71**, 1 (2008).
6. A. Noman Alhakimi,. "Synthesis, Characterization and Microbicides Activities of N-(hydroxy-4-((4-nitrophenyl) diazenyl) benzylidene)-2-(phenylamino) Acetohydrazide Metal Complexes." *Egypt. J. of Chem.* **63**, 4 (2020).
7. A. S. El-Tabl, M. ME Shakhdofo, A. A. Labib, and A. N. Al-Hakimi. "Antimicrobial activities of the metal complexes of N'-(5-(4-chlorophenyl) diazenyl)-2-hydroxybenzylidene)-2-hydroxybenzohydrazide." *Main Group Chem.* **11**, 4 (2012).
8. A. S. El-Tabl,., M. ME Shakhdofo, A. El-Seidy, and A. N. Al-Hakimi. "Synthesis, Characterization and Biological Studies of New Mn (II), Ni (II), Co (II), Cu (II) and Zn (II) of 2-(benzothiazol-2-yl)-N'-(2, 5-dihydroxybenzylidene) acetohydrazide." *J. of the Kor. Chem. Soc.* **55**, 1 (2011).
9. F. A. El-saied, , M. ME Shakhdofo, A. N. Al-Hakimi, and A. ME Shakhdofo. "Transition metal complexes derived from N'-(4-fluorobenzylidene)-2-(quinolin-2-yloxy) acetohydrazide: Synthesis, structural characterization, and biocidal evaluation." *Appl. Organ. Chem.* **34**, 11 (2020).
10. Ahmed N. Al-Hakimi, , F. Alminderej, L. Aroua, S. K. Alhag, M. Y. Alfai, J. A. Mahyoub, SE. I.

- Elbehairi, and A. S. Alnafisah. "Design, synthesis, characterization of zirconium (IV), cadmium (II) and iron (III) complexes derived from Schiff base 2-aminomethylbenzimidazole, 2-hydroxynaphthaldehyde and evaluation of their biological activity." *Arab. J. of Chem.* **13**,10 (2020).
11. M. ME Shakhdofo, F. A. El-Saied, and A. N. Al-Hakimi. "Synthesis, spectroscopic characterization and biological activity of 2-(p-toluidino)-N'-(2-hydroxybenzylidene) acetohydrazide complexes." *Main Group Chem.* **11**, 3 (2012).
 12. F. M. Alminderej, and L. Aroua, Design, Synthesis, Characterization and Anticancer Evaluation of Novel Mixed Complexes Derived from 2-(1H-Benzimidazol-2-yl) aniline Schiff base and 2-Mercaptobenzimidazole or 2-Aminobenzothiazole. *Egypt. J. of Chem.*, **64**(7) (2021).
 13. L. Aroua. "Synthesis and characterization of novel mixed complexes derived from 2-aminomethylbenzimidazole and 2-(1H-Benzimidazol-2-yl) aniline and theoretical prediction of toxicity". *Egypt. J. of Chem.*, **63**(12), (2020).
 14. F. M Alminderej, Synthesis, Design and Biological Evaluation of Antibacterial Activity of Novel Mixed Metal Complexes Derived from Benzoimidazolphenylethanamine and 6-Amino-N, N-dimethyluracil. *Lett. in Org. Chem.*, **18**(2), (2021).
 15. L. Aroua. Novel Mixed Complexes Derived from Benzoimidazolphenylethanamine and 4-(Benzoimidazol-2-yl) aniline: Synthesis, characterization, antibacterial evaluation and theoretical prediction of toxicity. *Asian J. of Chem*, **32**, (2020).
 16. S. S. Hussain, M. Ibrahim, S. Ambreen, M. Imran, M. Danish, and F. Sultana Rehmani. "Synthesis, spectral characterization, and biological evaluation of transition metal complexes of bidentate N, O donor Schiff bases." *Bioinorg. chem. and appl.* (2014).
 17. Vinita, Sh. Adsule, F. Ahmed, Zh. Wang, Z. Afrasiabi, E. Sinn, F. Sarkar, and S. Padhye. "Copper conjugates of nimesulide Schiff bases targeting VEGF, COX and Bcl-2 in pancreatic cancer cells." *J. of inorg. biochem.* **101**, 10 (2007).
 18. P Maria, W. Liu, A. Hagenbach, U. Abram, and R. Gust. "Synthesis, characterization and in vitro antitumour activity of a series of novel platinum (II) complexes bearing Schiff base ligands." *Eur. j. of med. chem.*, **53** (2012).
 19. P. Ashok, N. M Uttam Yadav, A. Pratik. Desai, and U. Pravin Singare. "Synthesis and antimicrobial activities of novel palladium (II) complexes of active Schiff's base ligand derived from 5-bromo isatin." *Inter. Lett. of Chem., Phys. and Astr.* **52** (2015).
 20. Ş. Ömer, Ü. Ö. Özdemir, N. Seferoğlu, Z. K. Genc, K. Kaya, B. Aydiner, S. Tekin, and Z. Seferoğlu. "New platinum (II) and palladium (II) complexes of coumarin-thiazole Schiff base with a fluorescent chemosensor properties: Synthesis, spectroscopic characterization, X-ray structure determination, in vitro anticancer activity on various human carcinoma cell lines and computational studies." *J. of Photo chem. and Photo bio. B: Bio.* **178** (2018).
 21. D. Sadia Afrin, F. Afsan, Md. Saddam Hossain, M. Nuruzzaman Khan, C. Zakaria, M. K. E. Zahan, and M. Ali. "A short review on chemistry of schiff base metal complexes and their catalytic application." *Inter. J. of Chem. Stu.* **6**, 3 (2018).
 22. R. Ramesh, P. K. Suganthy, and K. Natarajan. "Synthesis, spectra and electrochemistry of Ru (III) complexes with tetradentate schiff bases." *Synth. and React. in Inorg. and Met.-Org. Chem.* **26**, 1 (1996).
 23. V. Vasiliki, and M. Bakola-Christianopoulou. "Chemical Aspects of Organotin Derivatives of Beta-diketones, Quinonoids, Steroids and Some Currently Used Drugs: A Review of the Literature with Emphasis on the Medicinal Potential of Organotins." *Synth. and React. in Inorg., Met.-Org. and Nano-Met. Chem.* **37**, 7 (2007).
 24. P. Vigato Alessandro, V. Peruzzo, and S. Tamburini. "The evolution of β -diketone or β -diketophenol ligands and related complexes." *Coord. Chem. Rev.* **253**, 7-8 (2009).
 25. HA. Goss Carol, W. Henderson, L. Alistair Wilkins, and C. Evans. "Synthesis, characterisation and biological activity of gold (III) catecholate and related complexes." *J. of organo. chem.* **679**, 2 (2003).
 26. M. M. Abd El-Hady , and S. El-Sayed Saeed, Antibacterial Properties and pH Sensitive Swelling of Insitu Formed Silver-Curcumin Nanocomposite Based Chitosan Hydrogel , *Polyhedron.* **12**, 2451 (2020).
 27. El-Hady, A., Farouk, A., Saeed, S., & Zaghloul, S, Antibacterial and UV Protection Properties of Modified Cotton Fabric Using a Curcumin/TiO2 Nanocomposite for Medical Textile Applications. *Polymers*, **13**(22) (2021).
 28. L. Tzeng-Horng, and M. Chei Maa. "The molecular mechanisms for the antitumorogenic

- effect of curcumin." *Curr. Med.Chemistry-Anti-Cancer Age*, **2**, 3 (2002).
29. S. Keith, Ch. MacDonald, and M. Wallig. "Inhibition by rosemary and carnosol of 7, 12-dimethylbenz [a] anthracene (DMBA)-induced rat mammary tumorigenesis and in vivo DMBA-DNA adduct formation." *Cancer let.* **104**, 1 (1996).
 30. Kh. Roya Ranjineh, and S. Jalali Matin. "Synthesis, characterization, and antibacterial activities of some metal complexes of heptadentate schiff base ligand derived from acetylacetone." *Rus. J. of Appl. Chem.* **88**, 6 (2015).
 31. M. Aishatu Salihu, F. Abubakar, and A. Ebi Aye. "Synthesis, Characterization and Antifungal Activity of Manganese (II) Complex with Schiff Base Derived from Acetylacetone and Leucine." *Amer. J. of Nano Res. and Appl.* **5**, 6 (2017).
 32. A. I. Vogel, *Vogel's Text Book of Quantitative chemical Analysis*, John Wiley & Sons, New York (1989) pp 43-50.
 33. L. Lewis, R. G. Wilkins, *Modern Coordination Chemistry*, Interscience, New York (1960) pp 23,24 and 27.
 34. El-Saied, F. A., Salem, T. A., Shakdofa, M. M., & Al-Hakimi, A. N.. Anti-neurotoxic evaluation of synthetic and characterized metal complexes of thiosemicarbazone derivatives. *Appl. Organo. Chem.*, **32**(4) (2018).
 35. Th. A. Alorini, A. N. Al-Hakimi , S. El-Sayed Saeed , E. Hassan Lutf Alhamzi , A.E. Albadri, Synthesis, characterization, and anticancer activity of some metal complexes with a new Schiff base ligand ; *Arab. J. of Chem.* (2022).
 36. El Malti, Jazila, D. Mountassif, and H. Amarouch. "Antimicrobial activity of Elettaria cardamomum: Toxicity, biochemical and histological studies." *Food chem.* **104**, 4 (2007).
 37. H Fadwa, M. Akssira, A. Ezoubeiri, F. Mellouki, A. Benherraif, A. M. Blazquez, and H. Boira. "Chemical composition and antibacterial activity of essential oil of Pulicaria odora L." *J. of ethn.* **99**, 3 (2005).
 38. R Soma, K Rao, C. H. Bhuvanewari, A Giri, and L Narasu Mangamoori. "Phytochemical analysis of Andrographis paniculata extract and its antimicrobial activity." *World J. of Micro. and Bio.* **26**, 1 (2010).
 39. A. M. Mahboob, S. N. Abdulraheem, S. A. Almalki, A. A. Elhenawy, N. I. Alsenani, SE I. Elbehairi, A. M. Malebari, M. Y. Alfaifi, M. A. Alsharif, and S. YM Alfaifi. "Naproxen Based 1, 3, 4-Oxadiazole Derivatives as EGFR Inhibitors: Design, Synthesis, Anticancer, and Computational Studies." *Pharmaceuticals* **14**,9 (2021).
 40. Gh. Ayman A., M. Magdy El-Metwally, M. Shaaban, Sami A. Gabr, Nada S. Gabr, M. SM Diab, A. Aqel "Production of Terretinin N and Butyrolactone I by Thermophilic Aspergillus terreus TM8 Promoted Apoptosis and Cell Death in Human Prostate and Ovarian Cancer Cells." *Molecules* **26**, 9 (2021).
 41. G. William J. "The use of conductivity measurements in organic solvents for the characterisation of coordination compounds." *Coord. Chem. Rev.* **7**, 1 (1971).
 42. A. Noman Alhakimi, M. ME Shakdofa, S. Saeed, A. ME Shakdofa, M. S. Al-Fakeh, A. M. Abdu, and I. A. Alhagri. "Transition Metal Complexes Derived From 2-hydroxy-4-(p-tolyldiazenyl) benzylidene)-2-(p-tolylamino) acetohydrazide Synthesis, Structural Characterization, and Biological Activities." *J. of the Kor. Chem. Soc.* **65**,2 (2021).
 43. Al-Fakeh, M. S., Amiri, N., Al-Hakemi, A. N., Saeed, S. E. S., & Albadri, A. E. Synthesis and Properties of Two Fe(III) Coordination Polymers Based on 2-Amino-4-methylthiazole, 2-Mercaptobenzothiazole and Aromatic Polycarboxylate. *Asian J. Of Chem.*, **32**(10) (2020).
 44. A. Saad EL-Tabl , F. A. EL-Saied and A. Noman AL-Hakimi, Spectroscopic Characterization And Biological Activity Of Metal Complexes With An ONO Trifunctionalized Hydrazone Ligand, *J. Of Coord. Chem.* **61**, 15 (2008).
 45. R. R. Zaky, , K. M. Ibrahim, H. M. A. El-Nadar, and S. M. Abo-Zeid. "Bivalent transition metal complexes of (E)-3-(2-benzylidenehydrazinyl)-3-oxo-N-(p-tolyl) propanamide: Spectroscopic, computational, biological activity studies." *Spect. chim. Acta Part A: Mol. and Bio. Spect.* **150** (2015).
 46. A. Pedro E., M. P. dos Santos, S. Romera, and E. R. Dockal. "Synthesis, characterization, and spectroscopic studies of tetradentate Schiff base chromium (III) complexes." *Polyhedron* **26**, 7 (2007).
 47. A. N. Al-Hakimi, A. S. El-Tabl, and M. ME Shakdofa. "Coordination and biological behaviour of 2-(p-toluidino)-N'-(3-oxo-1, 3-diphenylpropylidene) acetohydrazide and its metal complexes." *J. of Chem. Res.* **2009**, 12 (2009).
 48. K. Irena, G. Momekov, T. Tzanova, and M. Karaivanova. "Synthesis, characterization, and cytotoxic activity of new lanthanum (III) complexes of bis-coumarins." *Bioinorg. chem. and appl.* **2006** (2006).

49. a) K. Nakamoto, in *Infrared and Raman Spectra of Inorganic and Coordination Compounds*. John Wiley & Sons, New York, **1997**. b) O. E. Offiong, E. Nfor, A. A. Ayi, , S. Martelli, *Trans. Met. Chem.* **25** (2000).
50. a) El-Saied, F. A., Salem, T. A., Shakdofa, M. M., Al-Hakimi, A. N., & Radwan, A. S.. Antitumor activity of synthesized and characterized Cu (II), Ni (II) and Co (II) complexes of hydrazone-oxime ligands derived from 3-(hydroxyimino) butan-2-one. *Beni-Suef University journal of basic and applied sciences*, 7(4) (2018). b) L. M. A. Jha, A. K. Yadaw, *Trans. Met. Chem.* **22** (1997).
51. M. Lallan, A. Jha, and A. K. Yadaw. "Synthesis, spectroscopic and antifungal studies of transition metal trinuclear/polynuclear complexes with azolo-2, 4-pentanedione: Part III." *Trans. Met. Chem.* **22**, 4 (1997).
52. Z. Hina, A. Ahmad, A. U. Khan, and T. Ali Khan. "Synthesis, characterization and antimicrobial studies of Schiff base complexes." *J. of Mol. Str.* **1097** (2015).
53. J. G. Collee, J. P. Duguid, A. G. Fraser, B. P. Marmion (Eds), *Practical Medical Microbiology*, Churchill Livingstone, New York, **1989**, pp. 89-96.
54. B. Hadariah, S. Solihah Khaidir, A. Mohd Tajuddin, K. Ramasamy, and B. M. Yamin. "Synthesis, characterization and anticancer activity of mono-and dinuclear Ni (II) and Co (II) complexes of a Schiff base derived from o-vanillin." *Polyhedron* **161** (2019).
55. D. Katja, M. Gold, L. Kober, F. Schmitt, L. Pfeifer, A. Dürrmann, H. Kostrhunova "Copper (II) complexes with tridentate Schiff base-like ligands: solid state and solution structures and anticancer activity." *Dal. Trans.* **48**, 40 (2019).
56. M. d Arafath Azharul, F. Adam, F. Saleih R. Al-Suede, M. R. Razali, M. B. Khadeer Ahamed, A. Malik Shah Abdul Majid, M. Zaheen Hassan, H. Osman, and S. Abubakar. "Synthesis, characterization, X-ray crystal structures of heterocyclic Schiff base compounds and in vitro cholinesterase inhibition and anticancer activity." *J. of Mol. Stru.* **1149** (2017).